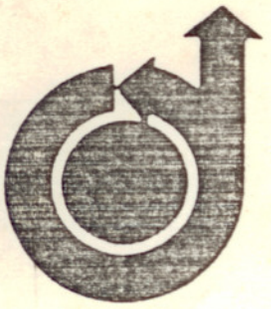

78-257

Thin Layer Approximation and Algebraic Model for Separated Turbulent Flows

B.S. Baldwin and H. Lomax, *NASA Ames Research Center, Moffett Field, Ca.*

AIAA 16TH AEROSPACE SCIENCES MEETING

Huntsville, Alabama/January 16-18, 1978

THIN-LAYER APPROXIMATION AND ALGEBRAIC MODEL FOR SEPARATED TURBULENT FLOWS

Barrett Baldwin* and Harvard Lomax**
Ames Research Center, NASA
Moffett Field, California 94035

Abstract

An algebraic turbulence model for two- and three-dimensional separated flows is specified that avoids the necessity for finding the edge of the boundary layer. Properties of the model are determined and comparisons made with experiment for an incident shock on a flat plate, separated flow over a compression corner, and transonic flow over an airfoil. Separation and reattachment points from numerical Navier-Stokes solutions agree with experiment within one boundary-layer thickness. Use of law-of-the-wall boundary conditions does not alter the predictions significantly. Applications of the model to other cases are contained in companion papers.

Nomenclature for Figures

a_∞ speed of sound in free stream

c chord length of airfoil

C_f skin-friction coefficient $2\tau_w/\rho_\infty u_\infty^2$

C_p pressure coefficient $2(p - p_w)/\rho_\infty u_\infty^2$

F_{MAX} maximum of function $F(y)$ (Eq. (8))

M_∞ free-stream Mach number

p_w pressure at the wall

p_t total pressure in free stream

p_∞ pressure in free stream

Re Reynolds number based on chord $\rho_\infty u_\infty c/\mu_\infty$

Re_x Reynolds number based on distance from leading edge $\rho_\infty u_\infty x/\mu_\infty$

Re_θ momentum thickness Reynolds number $\rho_\infty u_\infty \theta/\mu_\infty$

Re_{δ_o} Reynolds number based on boundary-layer thickness ahead of interaction $\rho_\infty u_\infty \delta_o/\mu_\infty$

u velocity parallel to solid surface

u_e velocity at edge of boundary layer

u_τ friction velocity $\sqrt{\tau_w/\rho_w}$

u_∞ free-stream velocity

y coordinate normal to solid surface

y^+ law-of-the-wall coordinate $\rho_w u_\tau y/\mu_w$

y_2^+ value of y^+ at computation point closest to wall

y_{MAX} value of y at which $F(y)$ (Eq. (8)) is maximum

α angle of attack of airfoil

δ boundary-layer thickness

δ_o boundary-layer thickness ahead of shock interaction

δ^* kinematic displacement thickness $\int_0^\delta (1 - u/u_e)dy$

θ momentum thickness $\int_0^\delta [\rho u(1 - u/u_e)/\rho_e u_e]dy$

τ local shear stress

τ_w shear stress at the wall

1. Introduction

There is a practical need in aeronautics as well as in other fields for the capability of calculating compressible turbulent separated flows. Although progress may have been made toward developing a universal (multiequation) turbulence model for use in such calculations, that goal has not yet been achieved (see e.g., Ref. 1 and references therein). On the other hand, with current numerical methods and available computers, investigators appear to be capable of analyzing quite general three-dimensional separated flows, if a suitable turbulence model were in existence. Completely satisfactory methods for treating turbulence may not be available in the near future. In the meantime it seems worthwhile to continue the development of procedures for calculating complicated flows based on simple empirical turbulence models.

The objective of this paper is to present results from an algebraic turbulence model developed for use in two- and three-dimensional Navier-Stokes machine codes. This model was used by Steger[2] to compute the flow over a biconvex airfoil, including a case in which buffeting occurred. It has also been used in preliminary three-dimensional calculations. In the present paper, properties of the solutions are investigated for an incident shock on a flat plate boundary layer, separated flow over a compression corner, and transonic flow over an airfoil.

2. Method

The basic equations for the numerical solutions under consideration are the Navier-Stokes equations. The effects of turbulence are simulated in terms of an eddy viscosity coefficient μ_t. Thus, in stress terms of the laminar Navier-Stokes equations, the molecular coefficient of viscosity μ is replaced by $\mu + \mu_t$. In heat flux terms $k/c_p = \mu/p_r$ is replaced by $\mu/p_r + \mu_t/p_{rt}$.

*Research Scientist. Member AIAA.
**Chief, Computational Fluid Dynamics Branch. Member AIAA.

Algebraic Turbulence Model

The algebraic turbulence model proposed in this paper is patterned after that of Cebeci[3] with modifications that avoid the necessity for finding the edge of the boundary layer. It is a two-layer algebraic eddy viscosity model in which μ_t is given by

$$\mu_t = \begin{cases} (\mu_t)_{inner} & y \leq y_{crossover} \\ (\mu_t)_{outer} & y_{crossover} < y \end{cases} \quad (1)$$

where y is the normal distance from the wall and $y_{crossover}$ is the smallest value of y at which values from the inner and outer formulas are equal.

The Prandtl-Van Driest formulation is used in the inner region

$$(\mu_t)_{inner} = \rho \ell^2 |\omega| \quad (2)$$

where

$$\ell = ky[1 - \exp(-y^+/A^+)] \quad (3)$$

$|\omega|$ is the magnitude of the vorticity

$$|\omega| = \sqrt{\left(\frac{\partial u}{\partial y} - \frac{\partial v}{\partial x}\right)^2 + \left(\frac{\partial v}{\partial z} - \frac{\partial w}{\partial y}\right)^2 + \left(\frac{\partial w}{\partial x} - \frac{\partial u}{\partial z}\right)^2} \quad (4)$$

and

$$y^+ = \frac{\rho_w u_\tau y}{\mu_w} = \frac{\sqrt{\rho_w \tau_w}\, y}{\mu_w} \quad (5)$$

The rationale behind the choice of the following relations will be discussed in later sections. In place of the Clauser formulation for the outer region

$$(\mu_t)_{outer} = KC_{CP}\rho F_{WAKE} F_{KLEB}(y) \quad (6)$$

where K is the Clauser constant, C_{CP} is an additional constant, and

$$F_{WAKE} = \left\{ \begin{matrix} y_{MAX} F_{MAX} \\ \text{or} \\ C_{WK}\, y_{MAX} U_{DIF}^2 / F_{MAX} \end{matrix} \right\} \text{ the smaller} \quad (7)$$

The quantities y_{MAX} and F_{MAX} are determined from the function

$$F(y) = y|\omega|[1 - \exp(-y^+/A^+)] \quad (8)$$

In wakes, the exponential term of Eq. (8) is set equal to zero. The quantity F_{MAX} is the maximum value of $F(y)$ that occurs in a profile and y_{MAX} is the value of y at which it occurs. The function $F_{KLEB}(y)$ is the Klebanoff intermittency factor given by

$$F_{KLEB}(y) = \left[1 + 5.5\left(\frac{C_{KLEB}\, y}{y_{MAX}}\right)^6\right]^{-1} \quad (9)$$

The quantity U_{DIF} is the difference between maximum and minimum total velocity in the profile (i.e., at a fixed x station)

$$U_{DIF} = (\sqrt{u^2 + v^2 + w^2})_{MAX} - (\sqrt{u^2 + v^2 + w^2})_{MIN} \quad (10)$$

The second term in U_{DIF} is taken to be zero (except in wakes).

The outer formulation (Eqs. (6) and (7)) can be used in wakes as well as in attached and separated boundary layers. The product $y_{MAX}F_{MAX}$ replaces $\delta^* u_e$ in the Clauser formulation and the combination $y_{MAX}U_{DIF}^2/F_{MAX}$ replaces δU_{DIF} in a wake formulation. In effect, the distribution of vorticity is used to determine length scales so that the necessity for finding the outer edge of the boundary layer (or wake) is removed.

The effect of transition to turbulence can be simulated by setting μ_t equal to zero everywhere in a profile for which the maximum tentatively computed value of μ_t from the foregoing relations is less than a specified value, that is,

$$\mu_t = 0 \quad \text{if} \quad (\mu_t)_{\substack{max\ in \\ profile}} < C_{MUTM}\mu_\infty \quad (11)$$

The constants appearing in the foregoing relations have been determined by requiring agreement with the Cebeci[3] formulation for constant pressure boundary layers at transonic speeds. The values determined are

$$A^+ = 26$$

$$C_{CP} = 1.6$$

$$C_{KLEB} = 0.3$$

$$C_{WK} = 0.25$$

$$k = 0.4$$

$$K = 0.0168$$

$$P_r = 0.72$$

$$P_{rt} = 0.9$$

$$C_{MUTM} = 14$$

Thin-Layer Approximation

The classical boundary-layer approximation is derived from the Navier-Stokes equations by retaining the lowest order terms in an expansion in inverse powers of Reynolds number. This formal procedure leads to (1) neglect of diffusion processes parallel to a body surface, and (2) replacement of the momentum equation normal to the surface with the assumption of zero normal pressure gradient throughout the boundary layer. The thin-layer approximation, on the other hand, neglects the diffusion processes parallel to a body surface but retains all three of the momentum equations and makes no assumptions about the pressure. One advantage of retaining the normal momentum equation comes about in applications to high Reynolds number, separated turbulent flows. Its use removes the troublesome singularities at the separation points and permits the straightforward computation of separated and reverse flow regions.

The development of the thin-layer approximation evolves directly from a realistic assessment

of what is really being computed in a typical high Reynolds number Navier-Stokes simulation. The layer of turbulent flow near the vorticity generating surface is so thin that typically a large amount of computer storage capacity is used in a highly stretched mesh to resolve the normal gradients of the flow there. As a result, in most, if not all, Navier-Stokes solutions of high Reynolds number turbulent flows that have been reported to date, the diffusion terms involving derivatives parallel to the surface simply have not been resolved[4] (even though an attempt may have been made to compute them) because of the lack of computer capacity. Stated in another way, most, if not all, Navier-Stokes solutions that make use of a highly stretched mesh near the body surface contain the thin-layer approximation whether or not they are coded to take advantage of it. The principal differences in the various codes lie in the way they model the removal of energy from the large-scale, computable structure, and the details of their approximation to the energy cascade in the body-normal direction.

The equations to be solved in a thin-layer approximation are based on time-averaged or subgrid scale models of the Navier-Stokes equations, but they are considerably less complicated than those based on approximations that attempt to use gradients parallel to the body surface to model turbulent and viscous diffusion in those directions. The simplifications in concept and numerical algorithm motivate the straightforward insertion of the approximation into computer codes for high Reynolds number flows. All solutions presented in this report are based on a thin-layer model, and all have been computed using the code developed by Steger.[2] In the calculations, the values of y_2^+ (Eq. (5)) at points nearest the wall were less than 2.0. Information on the numbers of mesh points and computation times is given in Table 1.

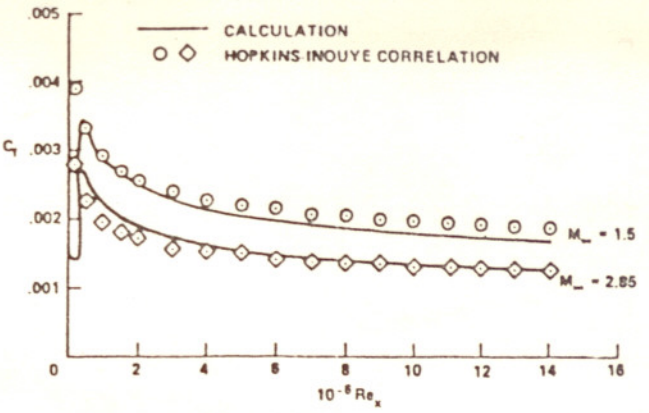

Fig. 1 Comparison of calculated skin friction on a flat plate with Hopkins-Inouye correlation.

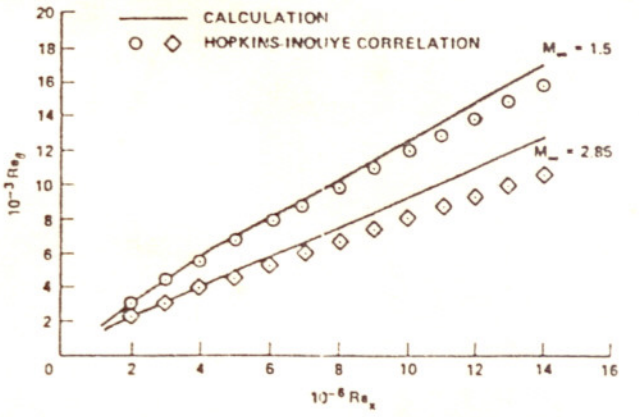

Fig. 2 Comparison of calculated momentum thickness on a flat plate with Hopkins-Inouye correlation.

3. Results

Flat Plate Boundary Layer

To help establish the validity of the method, Steger's[2] Navier-Stokes code was used to compute the boundary layer on a flat plate. In Fig. 1 the calculated skin friction is compared with the Hopkins-Inouye[5] correlation at Mach numbers of 1.5 and 2.85. With the constant $C_{MUTM} = 14$ in Eq. (11) the foregoing turbulence model predicts transition from laminar to turbulent flow (as indicated by the rise in skin friction) at a Reynolds number based on distance from the leading edge of about 300,000. In Fig. 2 the calculated momentum thickness Reynolds number is compared with results from the Hopkins-Inouye correlation. The comparisons in Figs. 1 and 2 indicate that the algebraic turbulence model of this paper produces values of skin friction and velocity profile shapes in reasonable agreement with experiment for equilibrium boundary layers.

Shock-Wave Incident on Flat Plate Boundary Layer

In Fig. 3 calculated surface pressure and skin friction are compared with the measurements of Reda and Murphy[6] for the interaction of a shock wave with the turbulent boundary layer on a flat plate. According to Rose[7] additional measurements for this flow are being made to determine the extent to which three-dimensional and unsteady effects influence the measurements. Because of the possible existence of such effects, it is not known how important the modifications of the turbulence models, which have

Table 1 Mesh points and computation times

	Number of mesh points	Number of time steps to convergence	Computation time on CDC 7600, sec	Code version
Shock-wave incident on flat plate	64 × 36	1800	1980	Jan. 1977
Flow over compression corner	64 × 36	1800	1980	Jan. 1977
Transonic airfoils	77 × 36	5200	6900	Jan. 1977
	77 × 36	1000	1400	July 1977

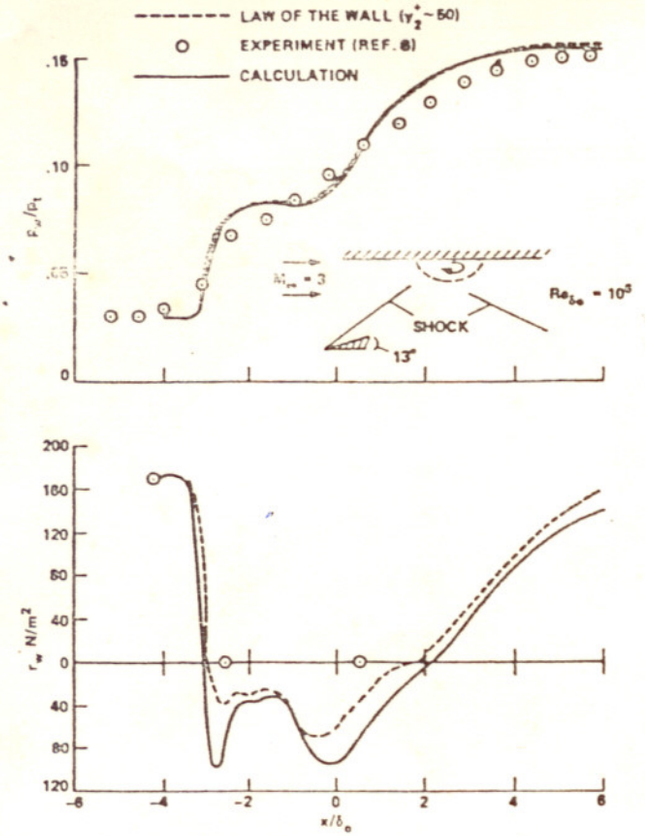

Fig. 3 Shock wave on flat plate boundary layer.

been considered[8-11] to accommodate these data, may be. In any case, the present predictions of the positions of separation and reattachment are within about one boundary-layer thickness of the measurements.

A word of explanation is in order about the fact that the present turbulence model predicts separation ahead of the experimental separation point, whereas previous calculations based on the Cebeci model predict separation much farther aft. Near the separation point, the function F(y) (Eq. (8)) develops a double peak and the inner peak is slightly larger. The inner peak occurs at a relatively small value of y_{MAX} such that F_{WAKE} (Eq. (7)) is small and the calculated eddy viscosity is suppressed, causing the predicted separation point to move forward.

Because some investigators recommend the use of law-of-the-wall boundary conditions, a calculation of that kind was carried out with the points closest to the wall at a distance corresponding to $y_2^+ \sim 50$ (Eq. (5)). The flow equations were solved analytically in the interval $0 \leq y \leq y_2$ for an adiabatic wall (with the conditions $\partial p/\partial y = 0$ and $\tau = \tau_w$ imposed) to obtain an expression for τ_w in the terms of the values of the flow quantities at $y = y_2$. Slip values of velocity and internal energy were then imposed at the wall such that the analytically determined value of τ_w and the adiabatic wall condition would result from the finite difference solution. In this procedure the expression for τ_w is implicit and involves a universal quadrature that depends on the turbulence model. Predictions from the resulting solution are included as dotted lines in Fig. 3. The calculated pressure distribution is not significantly altered by this approximation, but the predicted skin friction is noticeably affected. The difference is probably due to failure of the law-of-the-wall approximation $\tau = \tau_w$ and would increase with larger values of y_2^+.

Separated Flow over a Compression Corner

In Fig. 4 calculated surface pressure and skin friction are compared with measurements of Settles, Vas, and Bogdonoff[12] for a 24° compression corner. As in the previous case a double peak develops in F(y) (Eq. (8)) near separation resulting in a calculated separation point that is farther forward than is predicted by the Cebeci or Ames baseline model[10] (shown as a dotted line). The calculated region of reversed flow is too large and the predicted reattachment point differs by somewhat more than one boundary-layer thickness from the experiment. Judging from the effect of law-of-the-wall boundary conditions in the previous problem (Fig. 3), use of these conditions would perhaps enhance the comparison with experiment in this problem, although the calculation has not been carried out as yet.

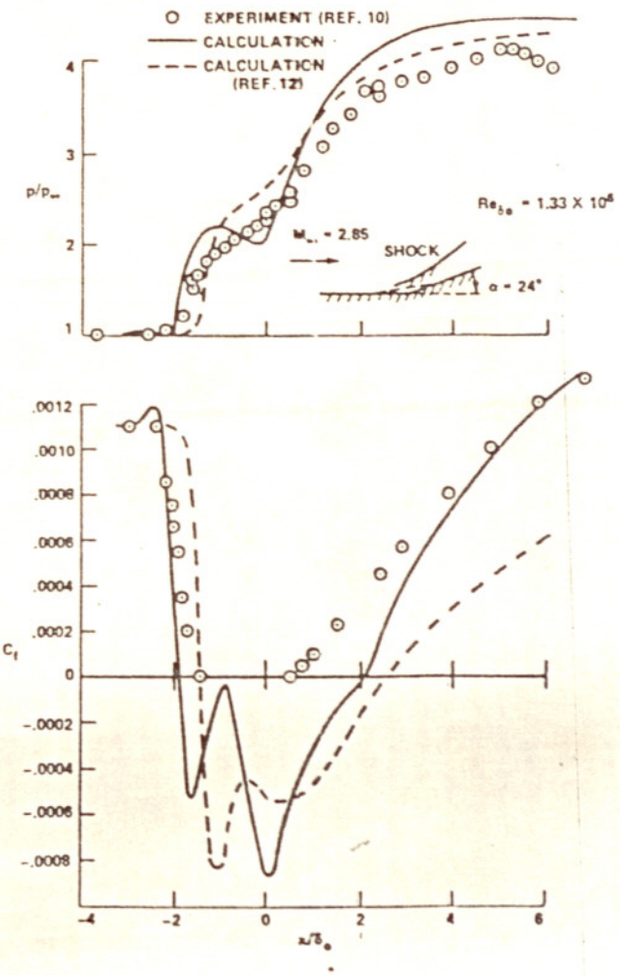

Fig. 4 Separated flow over a compression corner.

Transonic Airfoils

Figures 5-9 show details in the turbulent layers according to preliminary calculations of the flow over the Garabedian-Korn airfoil.[13] Figure 5 illustrates the reason for our use of $y_{MAX}F_{MAX}$ in the present algebraic eddy viscosity model in the place of $\delta^* u_e$, which is used in the Clauser and Cebeci formulations. The lower plot in Fig. 5 shows a velocity profile $u^+ = u/u_\tau$ versus y^+ (Eq. (5)) at a station near the nose of the airfoil. The edge of the boundary layer is at $y^+ \sim 500$. The middle plot shows the values of the product $\delta^* u_e$ that would be obtained from this profile if the edge of the boundary layer were taken to be at an arbitrary value of y (corresponding to y^+ in the scale at the bottom) rather than at the actual edge of the boundary layer. This shows the inaccuracies that can occur in the evaluation of eddy viscosity according to the Clauser formulation if the edge of the boundary layer is not accurately determined. In a machine code it is difficult to automate the determination of the edge of the boundary layer with precision, especially when sporadic values of velocity are computed due to the discretization. In contrast, the determination of F_{MAX} and y_{MAX} from the function $F(y)$ shown in the upper plot of Fig. 5 is much easier to automate because there is a well-defined maximum. In Fig. 5 the edge of the boundary layer corresponds closely to the peak in the middle plot, but this is not a good criterion for defining δ, as will be seen in Fig. 6.

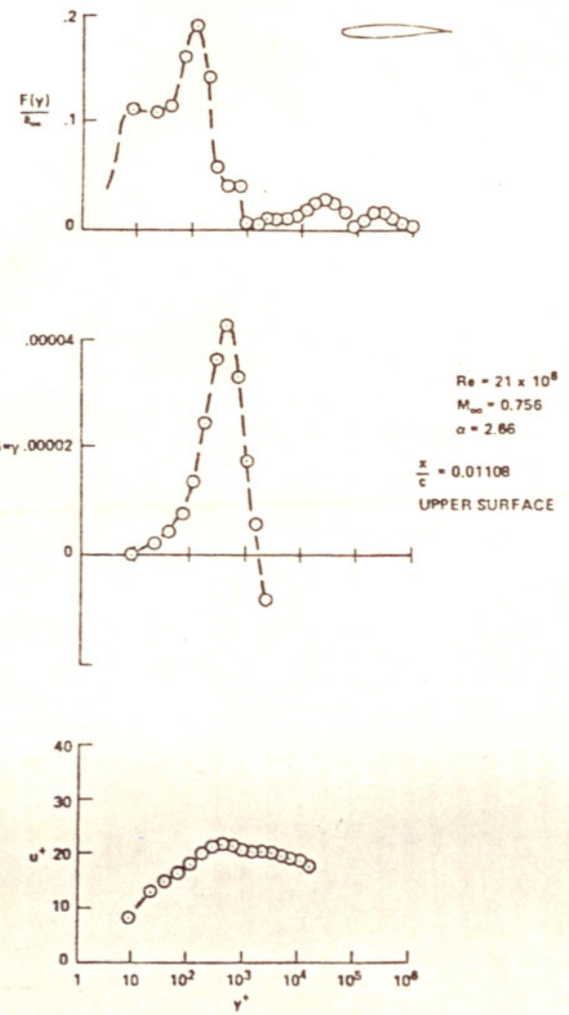

Fig. 5 Profiles near leading edge of Garabedian-Korn airfoil.

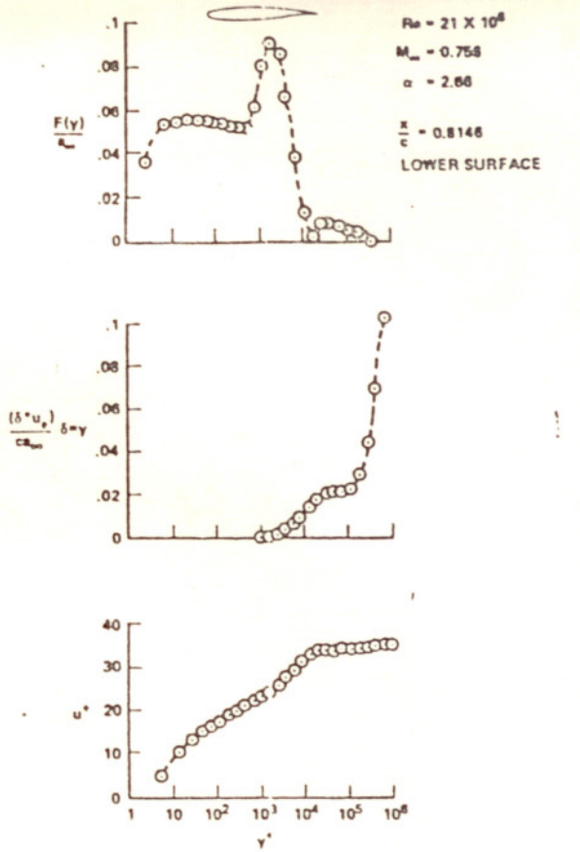

Fig. 6 Profiles near trailing edge of Garabedian-Korn airfoil.

Figure 6 contains the same kind of plots at a station near the trailing edge on the lower surface. In this case the edge of the boundary layer is at $y^+ \sim 30{,}000$. Again widely different values of $\delta^* u_e$ (middle plot) can be obtained if the edge of the boundary layer is incorrectly determined, whereas the maximum of $F(y)$ in the top plot is relatively well defined.

Figure 7 contains the same kind of plots at a station near the trailing edge on the upper surface where the flow is separated, as indicated by the negative values of u^+ in the lower plot. Another criterion that has been used for defining the edge of the boundary layer is based on the approach toward zero of the slope of the u versus y curve. However, spurious peaking of the u versus y curve outside the boundary layer due to discretization often invalidates this criterion. Also, in time-dependent calculations peaking can occur well inside the edge of the boundary layer.

It was found worthwhile to use a three-point quadratic fit in the determination of Y_{MAX} and F_{MAX} from the function $F(y)$ (see Figs. 5-7 and

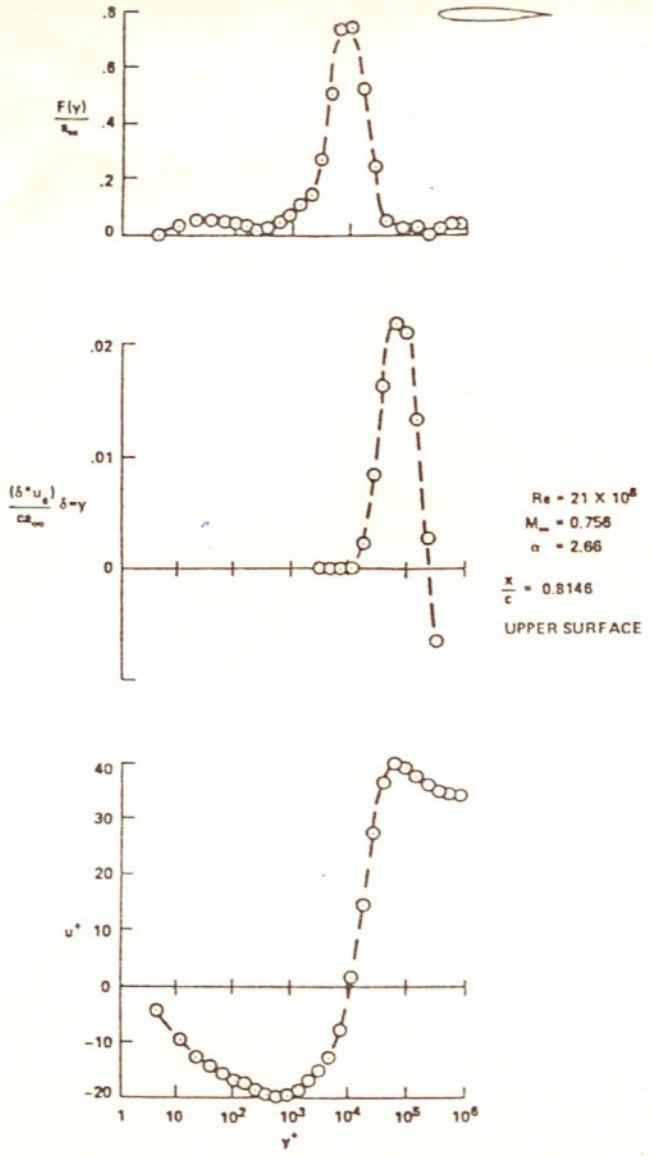

Fig. 7 Separated profile on Garabedian-Korn airfoil.

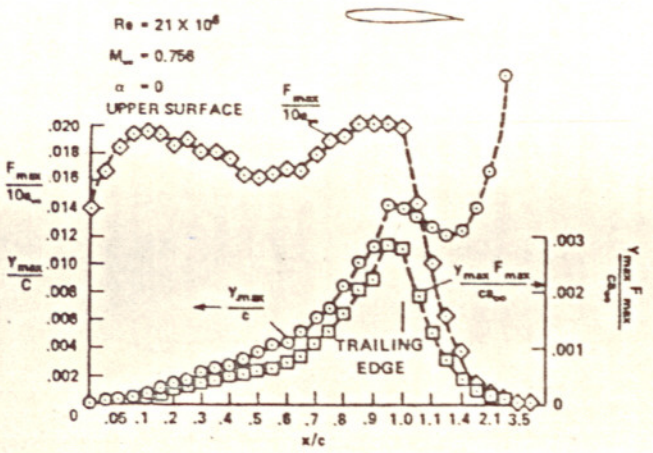

Fig. 8 Turbulence velocity and length scales on Garabedian-Korn airfoil.

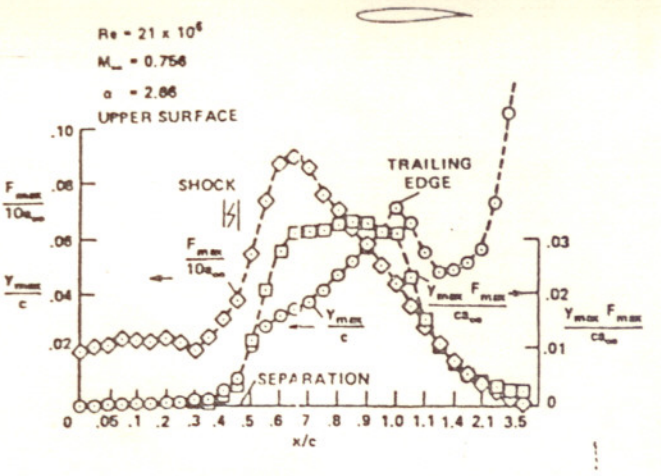

Fig. 9 Turbulence velocity and length scales on airfoil at angle of attack.

Eq. (8)). This procedure leads to smoother variations of Y_{MAX} and F_{MAX} from one profile to the next than are obtained when the discretized peaks of F(y) are used directly.

In Figs. 8 and 9 the variations of y_{MAX} and F_{MAX} along the upper surface are shown for the Garabedian-Korn airfoil at angles of attack of zero and 2.66°, respectively. There is a small amount of scatter of the calculated values about a mean line faired through the points. Our previous experience indicates that calculated values of $\delta^* u_e$ show much greater scatter so that smoothing over adjacent values of x is necessary as well as the imposition of arbitrary restrictions on the amount by which δ^* is allowed to vary from point-to-point. Thus, much of the arbitrariness in the calculated values of eddy viscosity in the outer part of the boundary layer is removed by adoption of the present turbulence model in place of that of Cebeci.[3] Figure 10 shows values of y_{MAX} and F_{MAX} on a biconvex airfoil.

In the foregoing treatment of transonic airfoils, transition was not included in the calculations (C_{MUTM} = 0 in Eq. (11)). Figure 11 contains

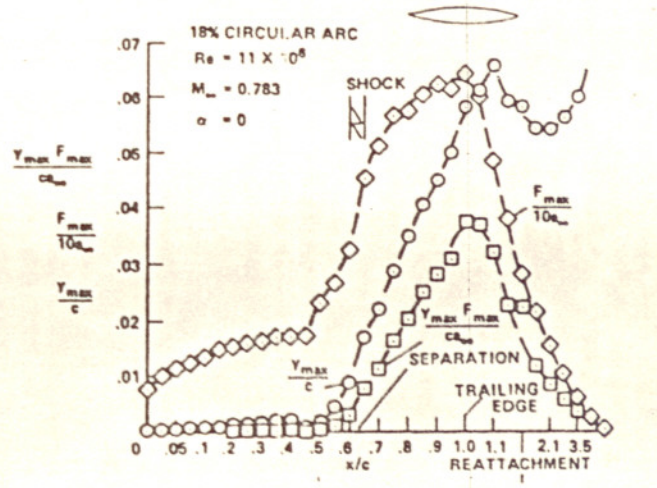

Fig. 10 Turbulence velocity and length scales on circular arc airfoil.

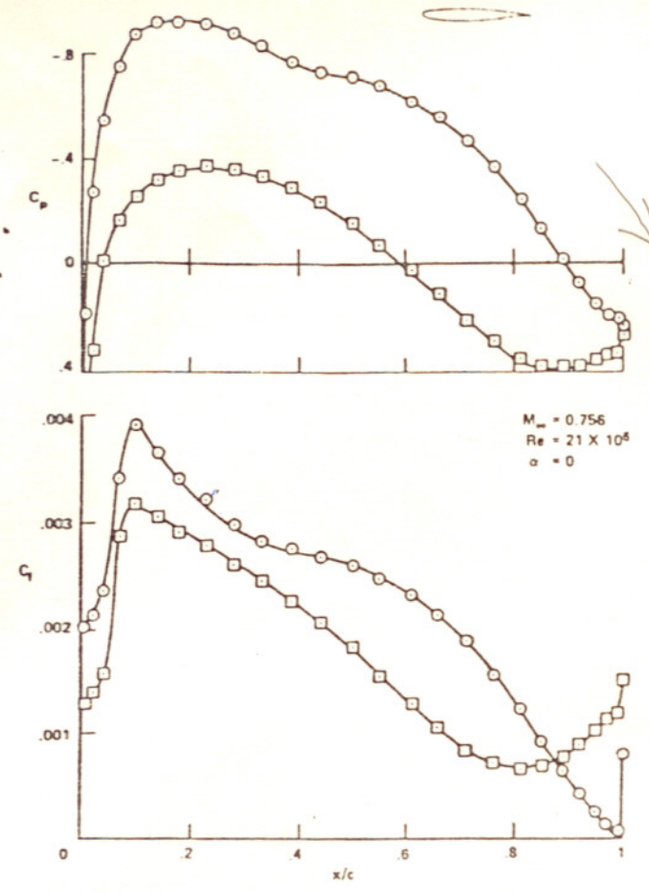

Fig. 11 Pressure and skin-friction distributions on Garabedian-Korn airfoil.

plots of pressure and skin-friction coefficients from calculations in which transition was considered with $C_{MUTM} = 14$. In the lower plot the abrupt rise in C_f near $x/c = 0.1$ indicates that for this value of C_{MUTM} transition is predicted to occur near the points where the negative C_p curves reach peaks on both upper and lower surfaces.

Uncertainties in Mach number and angle-of-attack correlations in the experiment hamper comparisons with the calculations. The experimental pressure distributions over a range of Mach numbers and angles of attack indicate the presence of a shock wave, on the upper surface near $x/c = 0.3$, that is not found in the calculation. Refinement of the mesh spacing in the x direction near the position of the shock is probably needed in the calculation. Although additional calculations are needed for worthwhile comparisons with the experimental pressure distributions, Fig. 11 is included in this paper to illustrate the properties of the turbulence model. The experimental drag coefficient is 0.0120 over a range of Mach numbers and angles of attack near zero and is 0.0091 from the calculation. The computed lift coefficient is 0.533; the coefficient that Kacprzynski et al.[13] believe corresponds to zero angle of attack at a Mach number of 0.739 is 0.53.

4. Conclusions

An algebraic eddy viscosity turbulence model has been developed that has several worthwhile properties. Its use eliminates the need for finding the edge of the boundary layer and thus removes one of the sources of arbitrariness and potential error that was present in previous Navier-Stokes solutions of separated turbulent flows based on zero or one-equation turbulence models. (The present method for defining length scales could also be used in one-equation models.) Comparisons with measurements from two experiments show agreement in the prediction of separation and reattachment points within about one boundary-layer thickness, as well as reasonable levels of skin friction aft of reattachment. Preliminary calculations of the flow over an airfoil indicate that the model is capable of dealing with relatively large shock-induced and trailing-edge separations. Comparisons with additional experiments and established knowledge of turbulent boundary layers are needed. These may indicate a need for variation with Reynolds number and Mach number of the values of the parameters that have been determined. The extent to which the thin-layer approximation is applicable in the presence of large shock-induced separations over airfoils needs further investigation. Applications to three-dimensional flows are being pursued. Use of the thin-layer approximation facilitates such applications. Possible use of law-of-the-wall boundary conditions to avoid resolution of the viscous sublayer should also be investigated to further simplify the three-dimensional calculations.

References

[1]Vegas, J. R. and Coakley, T. J., "Numerical Investigation of Turbulence Models for Shock-Separated Boundary Layer Flows," AIAA Paper 77-44, presented at AIAA 15th Aerospace Sciences Meeting, Los Angeles, Calif., Jan. 24-26, 1977.

[2]Steger, J. L., "Implicit Finite Difference Simulation of Flow About Arbitrary Geometries with Application to Airfoils," AIAA Paper 77-665, presented at AIAA 12th Thermophysics Conference at Albuquerque, New Mex., June 27-29, 1977.

[3]Cebeci, T., "Calculation of Compressible Turbulent Boundary Layers with Heat and Mass Transfer," AIAA Paper 70-741, presented at AIAA 3rd Fluid and Plasma Dynamics Conference, Los Angeles, Calif., June 29-July 1, 1970.

[4]MacCormack, R. W. and Baldwin, B. S., "A Numerical Method for Solving the Navier-Stokes Equations with Application to Shock-Boundary Layer Interactions," AIAA Paper 75-1, presented at AIAA 13th Aerospace Sciences Meeting, Pasadena, Calif., Jan. 20-22, 1975.

[5]Hopkins, E. J. and Inouye, M. I., "An Evaluation of Theories for Predicting Turbulent Skin Friction and Heat Transfer on Flat Plates at Supersonic and Hypersonic Mach Numbers," AIAA Journal, Vol. 9, No. 6, June 1971, pp. 993-1003.

[6]Reda, D. C. and Murphy, J. D., "Shock Wave Turbulent Boundary Layer Interaction in Rectangular Channels, Part II: The Influence of Sidewall Boundary Layers on Incipient Separation and Scale of Interaction," AIAA Paper 73-234, presented at AIAA 11th Aerospace Sciences Meeting in Washington, D.C., Jan. 10-12, 1973.

[7]Rose, W. C., private communication.

[8]Shang, J. S. and Hankey, W. L., "Numerical Solution for Supersonic Turbulent Flow over a Compression Ramp," AIAA Journal, Vol. 13, Oct. 1975, pp. 1368-1374.

[9]Baldwin, B. S. and Rose, W. C., "Calculation of Shock-Separated Turbulent Boundary Layers," Proceedings of Conference on Aerodynamic Analysis Requiring Advanced Computers, at Langley Research Center, Mar. 4-6, 1975, pp. 401-411.

[10]Horstman, C. C. and Hung, C. M., "Reynolds Number Effects on Shock-Wave Turbulent Boundary-Layer Interactions — A Comparison of Numerical and Experimental Results," AIAA Paper 77-42, presented at AIAA 15th Aerospace Sciences Meeting at Los Angeles, Calif., Jan. 24-26, 1977.

[11]Baldwin, B. S. and MacCormack, R. W., "Modifications of the Law of the Wall and Algebraic Turbulence Modelling for Separated Boundary Layers," AIAA Paper 76-350, presented at AIAA 9th Fluid and Plasma Dynamics Conference at San Diego, Calif., July 14-16, 1976.

[12]Settles, G. S., Vas, I. E., and Bogdonoff, S. M., "Details of a Shock-Separated Turbulent Boundary Layer at a Compression Corner," AIAA Journal, Vol. 14, No. 12, Dec. 1976, pp. 1709-1715.

[13]Kacprzynski, J. J., Ohman, L. H., Garabedian, P. R., and Korn, D. G., "Analysis of the Flow Past a Shockless Lifting Airfoil in Design and Off-Design Conditions," National Research Council of Canada Aeronautical Report LR-554, Nov. 1971.